

## Square-grid coordination networks of (5,10,15,20-tetra-4-pyridylporphyrinato)zinc(II) in its clathrate with two guest molecules of 1,2-dichlorobenzene: supramolecular isomerism of the porphyrin self-assembly

Rajesh Koner and Israel Goldberg\*

School of Chemistry, Sackler Faculty of Exact Sciences, Tel-Aviv University, Ramat-Aviv, 69978 Tel-Aviv, Israel  
Correspondence e-mail: goldberg@post.tau.ac.il

Received 8 February 2009

Accepted 17 February 2009

Online 25 February 2009

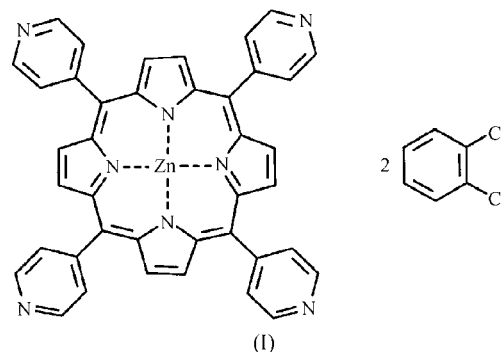
The title compound, (5,10,15,20-tetra-4-pyridylporphyrinato)zinc(II) 1,2-dichlorobenzene disolvate,  $[\text{Zn}(\text{C}_{40}\text{H}_{24}\text{N}_8)] \cdot 2\text{C}_6\text{H}_4\text{Cl}_2$ , contains a clathrate-type structure. It is composed of two-dimensional square-grid coordination networks of the self-assembled porphyrin moiety, which are stacked one on top of the other in a parallel manner. The interporphyrin cavities of the overlapping networks combine into channel voids accommodated by the dichlorobenzene solvent. Molecules of the porphyrin complex are located on crystallographic inversion centres. The observed two-dimensional assembly mode of the porphyrin units represents a supramolecular isomer of the unique three-dimensional coordination frameworks of the same porphyrin building block observed earlier. The significance of this study lies in the discovery of an additional supramolecular isomer of the rarely observed structures of metalloporphyrins self-assembled directly into extended coordination polymers without the use of external ligand or metal ion auxiliaries.

### Comment

The tetrapyridylporphyrin moiety in its free-base (TPyP) and metalated (MTPyP) forms is one of the most widely used building blocks in the design of porphyrin-based coordination networks. It has a planar and rigid structure, bearing laterally diverging pyridyl groups prone to coordination interaction with metal centres of neighbouring entities. There are two types of binding modes to this end. Thus, TPyP and MTPyP molecules may self-assemble readily through exocyclic metal ion nodes that can bridge between the lateral pyridyl sites of neighbouring units. A wide variety of such aggregation modes through diverse metal ion connectors have been reported (*e.g.* Abrahams *et al.*, 1994; Hagrman *et al.*, 1999; Sharma *et al.*,

1999; Carlucci *et al.*, 2003; Ohmura *et al.*, 2006). Alternatively, those MTPyP scaffolds in which the metal ion inserted into the porphyrin centre has an additional axial coordination capacity may self-associate into homogeneous polymeric arrays without resorting to external foreign ion auxiliaries. Here, the pyridyl groups of one porphyrin unit coordinate directly to the metal centres of adjacent porphyrin entities, leading to either one-, two- or three-dimensional multiporphyrin aggregates (Fleischer & Shachter, 1991; Krupitsky *et al.*, 1994; Lin, 1999; Diskin-Posner *et al.*, 2001; Pan *et al.*, 2002; George & Goldberg, 2005). The extended two- and three-dimensional coordination networks of the metalloporphyrins are of particular interest owing to their promising application in practical areas such as, for example, heterogeneous catalysis, molecular sieving and separation, as well as solid sensors. Indeed, the three-dimensional honeycomb coordination polymers of MTPyP were found to reveal attractive sorption and desorption features (Lin, 1999).

This study relates to the ZnTPyP compound and its direct self-assembly into coordination networks. In an earlier report (Krupitsky *et al.* 1994), we demonstrated the construction of isostructural three-dimensional single-framework ZnTPyP polymers with intralattice channels accommodated by water or a mixture of water and methanol. In that structure type [labelled as (II)], the zinc(II) ion is six-coordinate. Every porphyrin framework is bound axially to two adjacent units through the Zn atoms and equatorially to two additional porphyrins through two *trans*-related pyridyl substituents. A similarly structured acetic acid clathrate of ZnTPyP has been reported more recently (George & Goldberg, 2005). Another ladder-type one-dimensional coordination polymer composed of a mixture of five- and six-coordinate ZnTPyP moieties has also been reported (Diskin-Posner *et al.*, 2001). In the present investigation, we describe a two-dimensional mode of interporphyrin association of the ZnTPyP units, as observed in the title compound, (I). The latter represents a supramolecular



isomer of the three-dimensionally interconnected framework of type (II) described earlier. In (I), the ZnTPyP unit is located on a crystallographic inversion centre at  $(0, \frac{1}{2}, \frac{1}{2})$ , while the dichlorobenzene solvent resides in a general position (Fig. 1). The geometry around the zinc ion is octahedral, the axial positions being occupied by two pyridine N atoms of two adjacent ZnTPyP molecules (Table 1). The mutual orientation of the neighbouring porphyrins is roughly perpendicular, the dihedral angle between the mean planes of the respective

macrocyclic core rings (atoms C1–C10/N11/N12) being 79 (1)<sup>o</sup> (Fig. 2). The slight deviation from a strictly perpendicular mutual orientation of adjacent ZnTPyP units is reflected also in the nonlinear Zn1<sup>i</sup>··N16<sup>i</sup>··Zn1<sup>i</sup> [symmetry code: (i)  $x, -y + \frac{3}{2}, z + \frac{1}{2}$ ] angle of 153.55 (5)<sup>o</sup>. Then, the inclined approach of the axially coordinated pyridyl group to the zinc ion finds its mark in the sum of the bond angles around N16 to C15, C17 and Zn1( $-x, y + \frac{1}{2}, -z + \frac{1}{2}$ ) of 355.6<sup>o</sup>. The Zn··Zn distances in the multiporphyrin assembly are 9.981 (2) Å. The observed approximate square-grid porphyrin assembly is similar to the ‘paddle-wheel-like’ pattern found for the FeTPyP structure (Pan *et al.*, 2002). In the crystal, the ZnTPyP arrays are aligned parallel to the *bc* plane. As the self-assembly process took place in the presence of the dichlorobenzene solvent as a template, the two-dimensional coordination networks stack one on top of the other along the *a* axis in a parallel fashion, creating intralattice channel voids which accommodate molecules of the dichlorobenzene solvent (Fig. 2).

Fig. 3 shows a projection of the crystal structure of (I) down the *b* axis, and reveals the lipophilic interface between adjacent polymeric arrays and the tight steric fit between them. The interlayer stacking is thus mainly stabilized by dispersion forces. The important role of the dichlorobenzene solvent as templating agent in the creation of a clathrate-type structure can be appreciated by comparing the parallel stacking of the ZnTPyP coordination networks with the offset-stacked arrangements in a solvent-free structure of the FeTPyP flat polymeric arrays (Pan *et al.*, 2002). In the latter case, adjacent layers are shifted with respect to one another by about one-half of the grid size (approximately 7 Å). As a result, the pyridine rings pendant from the porphyrin entities in each FeTPyP layer effectively occupy the interporphyrin voids in the adjacent layers, without incorporating any additional solvent within the lattice.

As mentioned above, the supramolecular aggregation modes of ZnTPyP in (I) and in its earlier reported clathrates, exhibiting ZnTPyP assembly mode of type (II) (Krupitsky *et al.*, 1994; George & Goldberg, 2005), represent supra-

molecular isomers. As the two structure types crystallize concomitantly (see *Experimental*) from the crystallization mixture, the free energies of their formation should be comparable. In both structures, the coordination geometry around each Zn centre is octahedral, and every metalloporphyrin scaffold is coordinated to four adjacent units. The coordination geometries at every zinc site are almost identical in the two structure types. The central zinc ion binds axially from above and below to the pyridyl functions of two adjacent porphyrins, while two of the (*trans*-related) pyridyl groups coordinate to the metal centres of two other units. The two

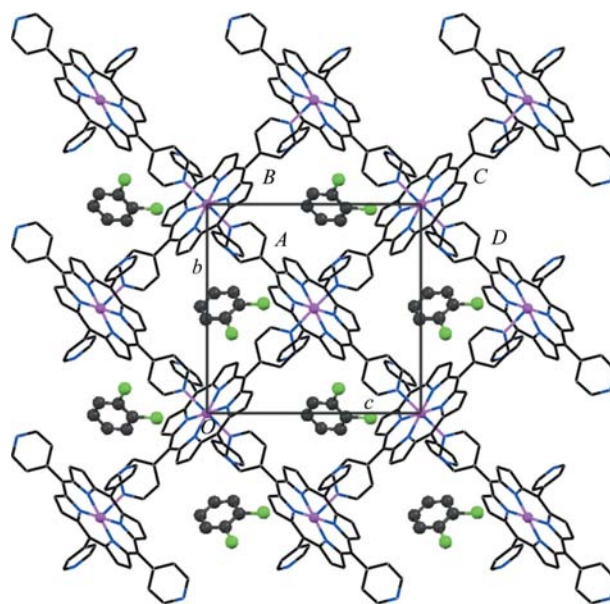


**Figure 2**  
A wireframe illustration of the square-grid coordination network of ZnTPyP, which is aligned parallel to the *bc* plane of the crystal. The dichlorobenzene solvent is accommodated within the interporphyrin voids. The Zn<sup>II</sup> ions in the porphyrin centre and the solvent species are depicted by small spheres and H atoms have been omitted. The labelling of the molecules as A, B, C and D is related to the discussion of the supramolecular isomorphism in the *Comment*. Note the parallel orientation of porphyrin cores B and C.

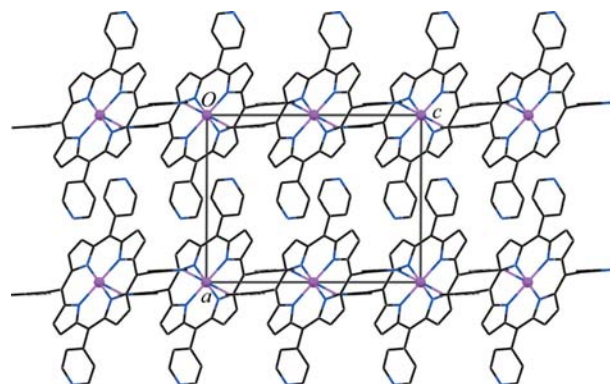


**Figure 3**  
A projection of the crystal structure down the *b* axis, showing the interface between the parallel-stacked coordination networks (seen edge-on). The Zn<sup>II</sup> ions are shown as small spheres, while the remaining structure has a wireframe representation. Solvent molecules and H atoms have been omitted.

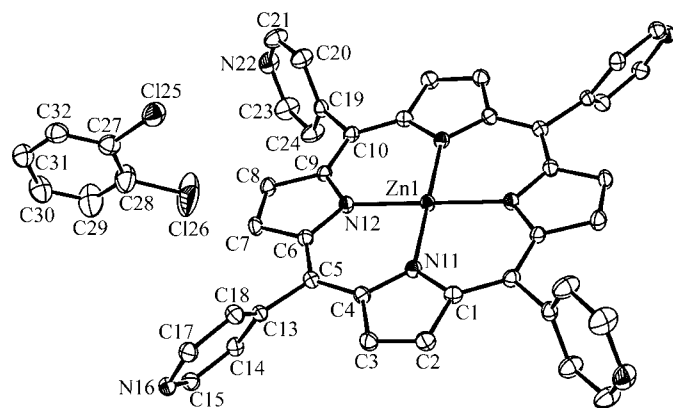


**Figure 1**  
The molecular structure of (I), showing the atom-labelling scheme. Ellipsoids represent displacement parameters at the 50% probability level at *ca* 110 K. The metalloporphyrin moiety resides on a crystallographic inversion centre at  $(0, \frac{1}{2}, \frac{1}{2})$ , and only atoms of the asymmetric unit are labelled. H atoms have been omitted.

other pyridyl arms of each porphyrin remain noncoordinated in either isomeric arrangement. The main difference between the two structures lies in the relative orientation of the coordinated porphyrins, a degree of freedom which arises from the possible rotation of one framework with respect to the other about the intermolecular Zn–N bond. A fragment of the porphyrin framework in structure type (II) is illustrated in Fig. 4 (Krupitsky *et al.*, 1994; George & Goldberg, 2005). Comparison of the spatial orientation of the assembled porphyrins reveals the following features. In the porphyrin framework of (I), molecules *A* and *B*, as well as *A* and *C* (as marked in Fig. 2), are nearly perpendicular to one another, while molecule *B* is parallel to *C* (and molecule *A* is parallel to *D*). On the other hand, in (II) porphyrin cores *B* and *C* are nearly perpendicular [rather than parallel as in (I)] to each other, the corresponding dihedral angle between their respective mean planes being  $83.5(5)^\circ$  (Fig. 4). The same applies to the next nearest neighbours *A* and *D* in (II). The actual structure that forms in a given experiment is affected by the crystallization environment. It appears that the three-dimensional coordination frameworking is preferred in hydrophilic solvents [such as water, acetic acid and small alcohols (Krupitsky *et al.*, 1994; Lin, 1999; George & Goldberg, 2005)]. In such cases, the noncoordinated pyridyl groups are solvated by the hydrophilic agent, inducing the trigonal structure type (II), where all the noncoordinated pyridyl groups line the walls of the interporphyrin channels formed

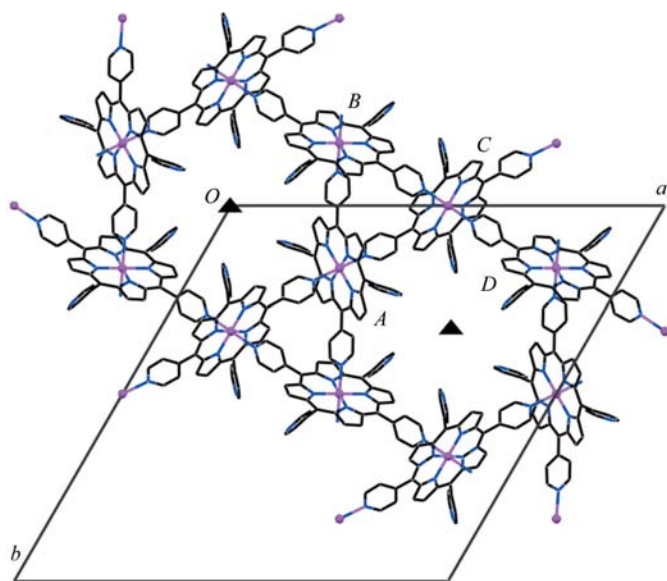


**Figure 4**

An illustration of the interporphyrin ZnTPyP coordination pattern of trigonal symmetry observed in the three-dimensional supramolecular isomer of type (II), which was reported previously (Krupitsky *et al.*, 1994; George & Goldberg, 2005); the projection of the crystal structure of the acetic acid clathrate is down the *c* axis (acetic acid molecules and H atoms have been omitted). The  $C_3$  axes are marked by solid triangles. Labelling of the molecules as *A*, *B*, *C* and *D* is related to the discussion of the supramolecular isomorphism in the *Comment*. The continuity of the shown framework in three dimensions is symbolized by the additional terminal  $Zn^{II}$  ions coordinated to the pyridyl group and the N-atom sites of neighbouring species coordinated to the zinc centres. Note the roughly perpendicular mutual orientation of porphyrin cores *B* and *C*.

around the trigonal axes. The solvent species are accommodated in these channels. In crystallization environments lacking foreign species that can interact with the ‘free’ N-atom sites of the pyridyl arms, the two-dimensional aggregation seems to be preferred, as in (I) and in FeTPyP. The ‘free’ pyridyl arms are then oriented towards the surface of the coordination layers (Fig. 3), being involved in dispersive aryl–aryl interactions between the layers.

In summary, compound (I) reveals an interesting self-coordinated two-dimensional network of ZnTPyP, with an almost square-grid geometry. It represents a supramolecular isomer of a three-dimensional coordination framework of ZnTPyP (Krupitsky *et al.*, 1994; George & Goldberg, 2005). Compound (I) is a clathrate-type structure, wherein the dichlorobenzene solvent is accommodated within intralattice channels created in the parallel-stacked arrangement of the coordination networks.

## Experimental

All reactants were obtained commercially. The procedure detailed below was intended to yield cocrystals of ZnTPyP with pyridine-3,5-dicarboxylic acid, with potential hydrogen bonding and/or coordination between the interacting components. However, it turned out that the dicarboxylic acid was not incorporated into the formed products. In the applied reaction, a solution of pyridine-3,5-dicarboxylic acid ( $1.5 \times 10^{-2}$  M, 4 ml) in dimethylformamide was carefully layered on to a solution of ZnTPyP ( $1.47 \times 10^{-3}$  M, 10 ml) dissolved in a 3:1 mixture of 1,2-dichlorobenzene and methanol. This mixture was left at room temperature for several days. The crystallized material was recovered by filtration, washed with dichlorobenzene and dried in air. Two types of crystals of different morphology were found: thin red needles and square blocks. The needle-shaped crystals were found to be isomorphous and isometric with the crystal structures of the methanol, water and acetic acid clathrates of ZnTPyP, wherein the metalloporphyrin moiety itself assembles in the form of a three-dimensional coordination framework (Krupitsky *et al.*, 1994; George & Goldberg, 2005). The square blocks of (I) represent a new material and are the subject of this report. IR (KBr,  $\text{cm}^{-1}$ ): 1593 (*m*), 1521 (*m*), 1486 (*w*), 1440 (*m*), 1342 (*m*), 1342 (*m*), 1204 (*w*), 1066 (*m*), 1010 (*m*), 993 (*s*), 795 (*s*), 753 (*s*), 717 (*m*), 705 (*s*), 670 (*m*).

### Crystal data

$[Zn(C_{40}H_{24}N_8)] \cdot 2C_6H_4Cl_2$	$V = 2157.39(7) \text{ \AA}^3$
$M_r = 976.03$	$Z = 2$
Monoclinic, $P2_1/c$	Mo $K\alpha$ radiation
$a = 11.0295(2) \text{ \AA}$	$\mu = 0.87 \text{ mm}^{-1}$
$b = 13.8207(2) \text{ \AA}$	$T = 110 \text{ K}$
$c = 14.1529(3) \text{ \AA}$	$0.30 \times 0.25 \times 0.15 \text{ mm}$
$\beta = 90.2383(7)^\circ$	

### Data collection

Nonius KappaCCD diffractometer	16059 measured reflections
Absorption correction: multi-scan (Blessing, 1995)	5115 independent reflections
$T_{\min} = 0.781$ , $T_{\max} = 0.881$	3970 reflections with $I > 2\sigma(I)$
	$R_{\text{int}} = 0.041$

### Refinement

$R[F^2 > 2\sigma(F^2)] = 0.044$	295 parameters
$wR(F^2) = 0.116$	H-atom parameters constrained
$S = 1.05$	$\Delta\rho_{\max} = 0.41 \text{ e \AA}^{-3}$
5115 reflections	$\Delta\rho_{\min} = -0.74 \text{ e \AA}^{-3}$

**Table 1**

Selected geometric parameters (Å, °).

Zn1–N11	2.0663 (16)	Zn1–N16 <sup>i</sup>	2.3393 (17)
Zn1–N12	2.0675 (17)		
N11–Zn1–N12	89.65 (7)	N12–Zn1–N16 <sup>i</sup>	87.73 (6)
N11–Zn1–N16 <sup>i</sup>	92.49 (6)		

 Symmetry code: (i)  $-x, y - \frac{1}{2}, -z + \frac{1}{2}$ .

H atoms were located in calculated positions and constrained to ride on their parent atoms, with C–H distances of 0.95 Å and  $U_{\text{iso}}(\text{H})$  values of  $1.2U_{\text{eq}}(\text{C})$ .

Data collection: *COLLECT* (Nonius, 1999); cell refinement: *DENZO* (Otwinowski & Minor, 1997); data reduction: *DENZO*; program(s) used to solve structure: *SIR97* (Altomare *et al.*, 1999); program(s) used to refine structure: *SHELXL97* (Sheldrick, 2008); molecular graphics: *ORTEPIII* (Burnett & Johnson, 1996) and *Mercury* (Macrae *et al.*, 2006); software used to prepare material for publication: *SHELXL97*.

This research was supported by The Israel Science Foundation (grant No. 502/08).

Supplementary data for this paper are available from the IUCr electronic archives (Reference: GD3276). Services for accessing these data are described at the back of the journal.

## References

- Abrahams, B. F., Hoskins, B. F., Michail, D. M. & Robson, R. (1994). *Nature (London)*, **369**, 727–729.
- Altomare, A., Burla, M. C., Camalli, M., Cascarano, G. L., Giacovazzo, C., Guagliardi, A., Moliterni, A. G. G., Polidori, G. & Spagna, R. (1999). *J. Appl. Cryst.* **32**, 115–119.
- Blessing, R. H. (1995). *Acta Cryst.* **A51**, 33–38.
- Burnett, M. N. & Johnson, C. K. (1996). *ORTEPIII*. Report ORNL-6895. Oak Ridge National Laboratory, Tennessee, USA.
- Carlucci, L., Ciani, G., Proserpio, D. M. & Porta, F. (2003). *Angew. Chem. Int. Ed.* **42**, 317–322.
- Diskin-Posner, Y., Patra, G. K. & Goldberg, I. (2001). *Dalton Trans.* pp. 2775–2782.
- Fleischer, E. B. & Shachter, A. M. (1991). *Inorg. Chem.* **30**, 3763–3769.
- George, S. & Goldberg, I. (2005). *Acta Cryst.* **E61**, m1441–m1443.
- Hagman, D., Hagman, P. J. & Jubieta, J. (1999). *Angew. Chem. Int. Ed.* **38**, 3165–3168.
- Krupitsky, H., Stein, Z., Goldberg, I. & Strouse, C. E. (1994). *J. Inclusion Phenom.* **18**, 177–192.
- Lin, K.-J. (1999). *Angew. Chem. Int. Ed.* **38**, 2730–2732.
- Macrae, C. F., Edgington, P. R., McCabe, P., Pidcock, E., Shields, G. P., Taylor, R., Towler, M. & van de Streek, J. (2006). *J. Appl. Cryst.* **39**, 453–457.
- Nonius (1999). *COLLECT*. Nonius BV, Delft, The Netherlands.
- Ohmura, T., Usuki, A., Fukumori, K., Ohta, T. & Tatsumi, K. (2006). *Inorg. Chem.* **45**, 7980–7990.
- Otwinowski, Z. & Minor, W. (1997). *Methods in Enzymology*, Vol. 276, *Macromolecular Crystallography*, Part A, edited by C. W. Carter Jr & R. M. Sweet, pp. 307–326. New York: Academic Press.
- Pan, L., Kelly, S., Huang, X. & Li, J. (2002). *Chem. Commun.* pp. 2334–2335.
- Sharma, C. V. K., Broker, G. A., Huddleston, J. G., Beldwin, J. W., Metzger, R. M. & Rogers, R. D. (1999). *J. Am. Chem. Soc.* **121**, 1137–1144.
- Sheldrick, G. M. (2008). *Acta Cryst.* **A64**, 112–122.